

## Accepted Manuscript

Title: Studies into the mass transfer and energy consumption of commercial feed spacers for RO membrane modules using CFD: Effectiveness of performance measures

Authors: Omid Kavianipour, Gordon D. Ingram, Hari B. Vuthaluru



PII: S0263-8762(18)30571-9  
DOI: <https://doi.org/10.1016/j.cherd.2018.10.041>  
Reference: CHERD 3411

To appear in:

Received date: 5 February 2018  
Revised date: 6 October 2018  
Accepted date: 30 October 2018

Please cite this article as: Kavianipour, Omid, Ingram, Gordon D., Vuthaluru, Hari B., Studies into the mass transfer and energy consumption of commercial feed spacers for RO membrane modules using CFD: Effectiveness of performance measures. Chemical Engineering Research and Design <https://doi.org/10.1016/j.cherd.2018.10.041>

This is a PDF file of an unedited manuscript that has been accepted for publication. As a service to our customers we are providing this early version of the manuscript. The manuscript will undergo copyediting, typesetting, and review of the resulting proof before it is published in its final form. Please note that during the production process errors may be discovered which could affect the content, and all legal disclaimers that apply to the journal pertain.

## Studies into the mass transfer and energy consumption of commercial feed spacers for RO membrane modules using CFD: Effectiveness of performance measures

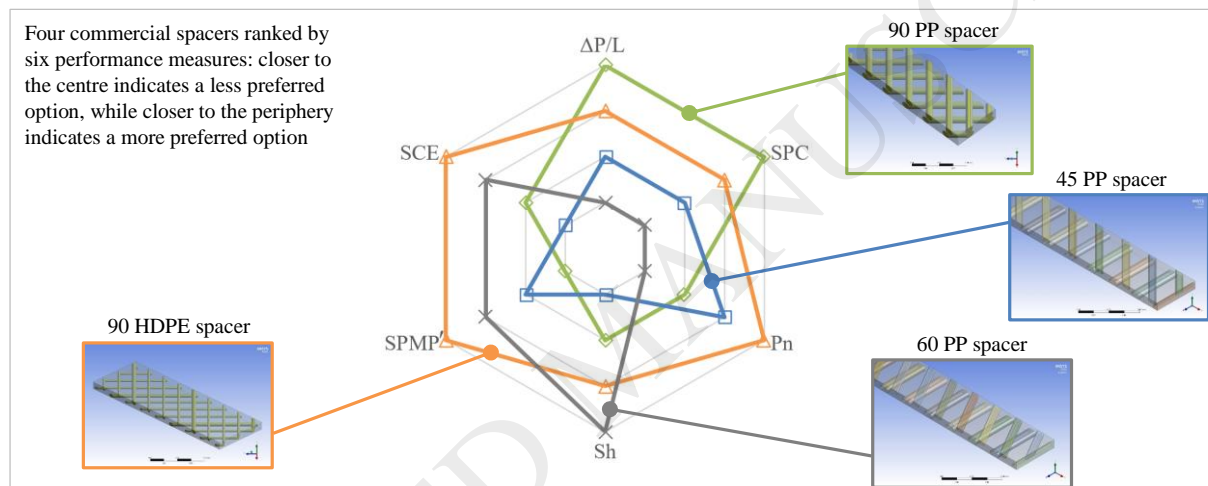
Omid Kaviani-pour, Gordon D. Ingram, Hari B. Vuthaluru <sup>1</sup>

WA School of Mines – Minerals, Energy & Chemical Engineering, Curtin University, GPO Box U1987, Perth, Western Australia 6845, Australia

<sup>1</sup>Corresponding author.

E-mail address: h.vuthaluru@curtin.edu.au (H.B. Vuthaluru).

### Graphical abstract



Note: Elsevier graphical abstracts should have 2:5 aspect ratio (<https://www.elsevier.com/authors/journal-authors/graphical-abstract>)

### Highlights

- Power law performance correlations have been formulated for four commercial feed spacers
- Different performance measures yield different spacer rankings at different flowrates
- The DelStar 90 HDPE spacer has good performance and a weak response to changing flowrate
- The SPMP performance measure does not show consistent behaviour with flowrate

### Abstract

Different approaches have been reported in the literature that aim to improve the performance of reverse osmosis (RO) desalination plant operations, attempting to make the desalination process more efficient.

This study investigates the performance of four commercial feed spacers for spiral wound reverse osmosis modules by considering energy consumption and production capacity, as well as their combination, through a previously proven approach to computational fluid dynamics (CFD) modelling.

Among the performance measures studied, SCE (spacer configuration efficacy), SPC (specific power consumption) and Pn (power number) showed a high level of predictability ( $R^2 \geq 0.998$ , 0.994 and 0.994, respectively) through power law correlations of Re with two spacer-dependent parameters. Of the four commercial spacers investigated, the DelStar Technologies Naltex N05013\_90HDPE-NAT (“90 HDPE”) spacer has been ranked as the best or second best based on multiple performance measures over the flow range  $Re = 50\text{--}100$ . Furthermore, the very weak response to flowrate changes observed for 90 HDPE, based on pressure loss, SPC, Pn, Sh and SCE measures, indicates the prospects for energy savings. SPMP', a modified definition of SPMP (Spacer Performance Ratio), shows no consistent response to flow variations for the spacers studied.

### Keywords

Membranes; Computational Fluid Dynamics (CFD); Reverse Osmosis (RO); Mass Transfer; Commercial Feed Spacer; Spacer Configuration Efficacy (SCE)

### Nomenclature

$a$	Discorectangle filament side length (m)
$A_{eff}$	Effective area ( $m^2$ )
$\Delta C_{Spacer}$	Difference in average concentration at inlet and outlet in spacer-filled channel (w/w)
$\Delta C_{Slit}$	Difference in average concentration at inlet and outlet in open channel (w/w)
$d$	Filament diameter (m)
$D_h$	Hydraulic diameter (m)
$h$	Discorectangle filament height (m)
$H$	Channel height (m)
$L$	Channel length (m)
$\Delta P/L$	Pressure drop per unit length (Pa/m)
$\Delta P_{Spacer}$	Difference in average pressure at inlet and outlet in spacer-filled channel (Pa)
$\Delta P_{Slit}$	Difference in average pressure at inlet and outlet in open channel (Pa)
Pn	Power number
$r$	Discorectangle filament radius (m)
$Re_{ch}$	Channel Reynolds number
$Re_h$	Hydraulic Reynolds number
SCE	Spacer Configuration Efficacy
Sh	Sherwood number

SPC	Specific Power Consumption ( $\text{W}/\text{m}^3$ )
SPMP	Spacer Performance Ratio introduced by (Schwinge et al., 2002)
SPMP'	Spacer Performance Ratio based on constant feed mass flowrate
$u_{eff}$	Effective velocity (m/s)

#### *Greek symbols*

$\varepsilon$	Porosity
---------------	----------

## 1. Introduction

Reverse osmosis (RO) operations consume the minimum amount of energy per unit product in comparison to other desalination processes such as multi-stage flash, multi-effect distillation and mechanical vapour compression (UNESCO, 2015). However, RO operations still consume about three times the minimum theoretical required energy (Dashtpour and Al-Zubaidy, 2012), which provides opportunities for optimization in this area. This optimization could be achieved by the appropriate design and manufacturing of the membrane or through optimization of feed spacer configurations leading to enhanced mass transfer and lower energy consumption.

Market studies have shown that since the 1990s, Spiral Wound Modules (SWMs) have become the major membrane configuration used in RO operations. Most plants that used Hollow Fine Fibre Modules, the other major technology at that time, now use SWMs instead, which has resulted in significant cost savings (Jon Johnson, 2009).

Over the two decades leading to 2008, SWM technology has benefited from both spacer and membrane improvements. For example, the capacity of 20 cm (8 inch) commercial SWMs has doubled while their salt passage has reduced to about one third. The development of 40 cm (16 inch) modules and an increase in the operating pressure from 6.9 MPa (1000 psi) to 8.3 MPa (1200 psi) has further enhanced SWMs (Jon Johnson, 2009).

In SWMs, every feed layer neighbours two permeate layers and every permeate layer is surrounded by two feed layers. In most configurations, spacers are used on both feed and permeate sides, but they fulfil different roles during operation. Because of the higher pressure on the feed side, permeate spacers ensure that the membranes are not squeezed together and that the permeate flow pathway is kept open. On the other hand, feed spacers are meant to break down the concentration polarization layers on the feed side. Providing better mixing on the feed side will reduce the concentration at the membrane surface, thus minimizing the static osmotic pressure at the membrane.

There is a well-recognized relationship between mass transfer and pressure drop in RO modules (Cipollina et al., 2009; Cipollina et al., 2011; Fimbres-Weihs and Wiley, 2007; In Seok and Ho Nam, 1982; Kaviani-pour et al., 2017; Li et al., 2002a; Li et al., 2002b, 2004; Qureshi and Shakaib, 2013; Saeed, 2012; Saeed et al., 2013; Saeed et al., 2015a, b; Saeed et al., 2012; Schock and Miquel, 1987), which results in a trade-off between production rate and production costs. Over the last two decades, no significant benefits have been realised from the optimization of commercial spacers, despite all efforts to enhance their performance (Jon Johnson, 2009). This could be attributed to several factors, including lack of computational resources, low accuracy of models as a result of simplified or unrealistic assumptions, emphasis on either mass transfer or energy consumption instead of considering both, lack

of a consistent method for quantifying the effect of recirculation and dead zones on performance and maintenance costs, and/or there being simply no room for further improvement in feed spacer designs.

Since the 1970s, different methods have been used to characterize the performance of RO units. Some of them focussed on pressure drop, while the others addressed production rate. In 2002, the Spacer Performance Ratio (SPMP) was introduced (Schwinge et al., 2002). Significantly, it combined both aspects of performance, but it did not receive any further attention. No new combined approach was reported until 2012, when the Spacer Configuration Efficacy (SCE) concept was proposed (Saeed et al., 2012) and applied to the optimization of Ladder-type spacers (Saeed et al., 2013; Saeed et al., 2015b). Both SPMP and SCE aim to address the disadvantages of older approaches. However, no further studies have been carried out either to investigate or compare their effectiveness in predicting the performance of spacers until our recent work (Kavianipour et al., 2017) in which we studied four conventional spacer geometries. Apart from these studies, there was no attempt from researchers to investigate the accuracy and improve the quality of spacer performance measures.

SWM manufacturers generally do not provide practical, detailed information about their product performance. The module datasheets usually include penetration rate, minimum salt rejection rate, maximum applied pressure and maximum pressure drop. However, it is usually not clear whether all these parameters are linked to a single operational case or different cases, or even if they reflect practical conditions or design limits. No further information is available in typical datasheets to provide indications for the estimation of the performance of spacers in different operational conditions.

In the current study, SCE, SPMP' and other performance measures are used to compare four commercially available feed spacers. In addition, the SCE and SPMP' concepts are analysed using different methods to gain further insights into the effectiveness of commercial spacers. Reducing energy requirements while maintaining production capacity are longstanding research themes, but no previous study has explored the effectiveness of commercial spacers using performance measures, like SCE and SPMP', that combine energy consumption and production capacity in a single measure. The results reported on the effectiveness of commercial spacers are new and of practical relevance to the design of membrane modules and the operation of RO systems.

## **2. Simulation approach**

### *2.1. Geometries studied*

In the present work, four different commercial spacers provided by DelStar Technologies are studied. The spacers are from the Naltex family and are denoted N05013\_90HDPE-NAT (90 HDPE), N06006/06\_45PP-NAT (45 PP), N06407\_90PP-NAT (90 PP) and N08006\_60PP-NAT (60 PP). Figure 1 shows a part of the fluid flow domain and the geometries of the different spacers. The specifications supplied by the manufacturer include the number of filaments per inch, spacer heights and angle of attack, but provide no information about the filament shape or dimensions.

In this study, all the spacer dimensions were measured with appropriate tools from feed spacer samples. The filament cross-sectional shapes for 90 HDPE and 90 PP were assumed to be circular, while 60 PP and 45 PP had discorrectangle-shaped filaments with the straight length equal to the diameter. All filaments were straight in the longitudinal direction. Details of the geometrical parameters of the spacers are given in Table 1.

### *2.2. Parameters considered for simulation*

Spacer Performance Ratio (SPMP), defined below, characterizes the ratio of ‘mass transfer enhancement caused by spacer’ over ‘pressure drop increase caused by spacer’ (Schwinge et al., 2002).

$$\text{SPMP} = \frac{\frac{\Delta C_{\text{Spacer}}}{\Delta C_{\text{Slit}}}}{\frac{\Delta P_{\text{Spacer}}}{\Delta P_{\text{Slit}}}}$$

As clarified in recent communications with the authors [D. Fletcher, personal communication, 2017], the same  $Re_{ch}$  was used in the original work when simulating concentration and pressure changes with a spacer and without (denoted by ‘Slit’ in the definition above). To eliminate the effect of the channel porosity and to make it more general, it has been decided in the current work to use the same feed mass flowrate for both empty channel and spacer cases, rather than using the same  $Re$ . Therefore, the difference between spacer and slit scenarios is the presence or absence of the spacer, with all other parameters being the same. This modified performance measure is denoted SPMP’.

All other parameters used in this study, including hydraulic diameter ( $D_h$ ), effective velocity ( $u_{eff}$ ), effective area ( $A_{eff}$ ), porosity ( $\epsilon$ ), Reynolds number ( $Re$ ), specific power consumption (SPC), power number ( $Pn$ ), Sherwood number ( $Sh$ ) and spacer configuration efficacy (SCE) have been defined and discussed in our previous work (Kavianipour et al., 2017).

### 2.3. Governing equations, modelling software and solution options

The Navier-Stokes equations are used to describe the conservation and transport processes occurring in the feed side membrane channel. The fluid was assumed to be Newtonian and incompressible, while the flow was assumed to be steady-state, laminar, no slip and isothermal. Fixed values were used for the solute mass fraction at the inlet and at the membrane surface, a no flux boundary condition was employed for the filament and symmetry surfaces, and the solute mass diffusivity was taken to be constant. The governing continuity, momentum and species conservation equations, along with hardware and software parameters, are clarified in our previous work (Kavianipour et al., 2017).

In the present study, different ANSYS 15.0, 16.0 and 17.0 modules were used to model flow through the feed channels, including ANSYS Geometry, ANSYS Meshing, ANSYS Fluent and ANSYS Workbench.

The Coupled Scheme chosen in the ANSYS Fluent solver as it offers steady convergence with minimal fluctuations through the iterations. For spatial discretization, the Green-Gauss Node Base method was used for Gradient, Second Order for pressure, Third-Order MUSCL for momentum and Power Law for salinity calculations. The maximum accepted error was set to  $10^{-5}$ .

### 2.4. Domain, mesh generation and simulation parameters

Domain definition, geometrical approximations of filaments near the membrane and other filaments, mesh generation procedures and different parameters used in the simulation are all described in our previous work (Kavianipour et al., 2017). The mesh sizes used for the four spacers are presented in Table 1.

## 3. Results and discussion

Simulation runs, covering 16 cases, were performed using ANSYS Fluent. All calculated performance measures, such as SPC,  $Pn$  and SPMP’, are based on the weighted average values extracted from the software. Parametric effects on the performance of the commercial spacers are reported below.

### 3.1. Effect of Reynolds number

The current work aims to evaluate and compare the effectiveness of different spacers over a range of feed rates. Different approaches to characterize the feed flowrate are used in the literature, including

mass flowrate, average velocity and Reynolds number. Hydraulic Reynolds number was chosen to make it possible to compare the results with other commercial spacers, which have different channel heights and porosities. All models were run at Re values of 50, 100, 150 and 200, except for 60 PP for which the flow becomes turbulent at lower-than-usual Re, making it unsuitable for modelling with laminar flow equations in steady-state mode. To keep the results comparable, 60 PP was studied for Re values of 50, 75, 100 and 125, where the flow remains laminar.

Table 2 presents a summary of the simulation results in the form of power law equations and provides a clear comparison of the different configurations. A custom-written MATLAB® program was used to optimize the power law parameters to yield the maximum coefficient of determination ( $R^2$ ) for every data set. Together with the equations, Table 2 also presents the lowest value of  $R^2$  for each correlation for the four spacers. Comparison of the power law equations and the CFD results is shown in Figures 2–6 and 8, with symbols representing the CFD results and lines representing the power law correlations. To facilitate comparison of the new results in Table 2 with our previous work, selected results from (Kavianipour et al., 2017) are reproduced in Table 3.

### 3.1.1. Pressure drop

In agreement with other studies (Cipollina et al., 2009; Cipollina et al., 2011; Fimbres-Weihs and Wiley, 2007; In Seok and Ho Nam, 1982; Li et al., 2002a; Li et al., 2002b, 2004; Qureshi and Shakaib, 2013; Saeed, 2012; Saeed et al., 2013; Saeed et al., 2015a, b; Saeed et al., 2012; Schock and Miquel, 1987), Figure 2 **Error! Reference source not found.** indicates that for all geometries, the pressure drop per unit length increases with Re.

Table 2 shows that the pressure drop is proportional to  $Re^{1.4-2.0}$  depending on the spacer geometry. The power law exponent is in the expected range, but is slightly higher than reported previously Table 3 for more simple geometries ( $Re^{1.29-1.55}$ ). This means that the commercial spacers are more responsive to flow changes, and will experience larger relative increase in pressure drop with flowrate, compared to the more simple geometries. The commercial spacers would provide more benefit, with respect to change in pressure drop, from being used in the lower range of Re values.

As shown in Figure 2, 90 PP has the lowest pressure drop for low flowrates ( $Re < 120$ ) but, owing to its strong relation with Re ( $\propto Re^{2.02}$ ), for higher flowrates, it loses this position, with 90 HDPE showing the lowest pressure drop according to its weaker relation to Re ( $\propto Re^{1.39}$ ).

On the other hand, comparing the values of pressure drop for different spacers, including the four simple geometries studied in (Kavianipour et al., 2017), reveals that for  $Re = 200$ , spacers show comparable values when categorized into three groups: simple spacers (Ladder-type, Triple, Wavy and Submerged, termed the “base group”), commercial spacers (90 PP, 45 PP, 90 HDPE and 60 PP) and a plain open channel.

- Simple spacers have a pressure drop in the range 9–11 kPa/m;
- Commercial spacers have 2–10 times greater pressure drop compared to the base group;
- The plain channel has 15% of the base group pressure drop.

In addition, it is notable that the 90 HDPE spacer has the lowest power law exponent among the four, which could be a result of having three small filaments ( $d = 0.3H$ ) after every normal-sized filament ( $d = 0.5H$ ) as seen in Figure 1(d). This will increase the porosity of the channel and provide a higher cross-sectional area for fluid passage. These small filaments cause the flow to act differently at low and high flowrates. This matter is discussed in more detail in Section 3.2.

### 3.1.2. Power consumption

Similar to our previous work and other studies, Figure 3 shows that SPC increases significantly with increasing flowrate. The 90 PP spacer has the lowest SPC for Reynolds numbers less than 110, while for  $Re > 110$ , 90 HDPE has the lowest SPC. On the other hand, 60 PP has the highest SPC over the Re range studied. The highest rate of increase in SPC is for the 90 PP geometry, which has  $SPC \propto Re^{2.85}$ , while the lowest is for 90 HDPE, for which  $SPC \propto Re^{2.42}$  (Table 2).

Including the results from our previous work (Table 3), it is notable that the power law exponent for SPC varies in a narrower range than for pressure drop (2.32–2.85 for SCE compared to 1.29–2.02 for pressure drop) among all eight spacer-filled channels investigated.

The relationship between Pn and Re is shown in Figure 4 and is consistent with the SPC results for the 90 HDPE, 45 PP and 60 PP spacers. Because  $Pn \propto SPC \times H^4$ , it is very sensitive to channel height. The channel height of 90 PP is greater than for the other spacers, which explains why its Pn results are higher than those of the other spacers.

In addition, similar to pressure drop, the three categories of spacers display different Pn ranges. The Pn values of commercial spacers are an order of magnitude greater than those of the simple spacers, which in turn are an order of magnitude greater than the Pn of a plain channel.

### 3.1.3 Mass transfer

Figure 5 shows Sh results for different flowrates and spacers. Previous studies revealed that mass transfer and Sherwood number increase with Re (Da Costa et al., 1994; Fimbres-Weihs and Wiley, 2007; In Seok and Ho Nam, 1982; Kavianipour et al., 2017; Li et al., 2002a; Li et al., 2002b, 2004; Saeed, 2012; Saeed et al., 2013; Saeed et al., 2015a, b; Saeed et al., 2012; Santos et al., 2007; Schock and Miquel, 1987; Schwinge et al., 2002). Some of these studies attempt to quantify that relation and reported equations linking Sh and Re for different geometries (Da Costa et al., 1994; In Seok and Ho Nam, 1982; Kavianipour et al., 2017; Schock and Miquel, 1987).

In all cases, the recommended equations are in the form of a power law in which the exponent is positive and less than one. Of the four geometries studied in this work, 60 PP has the highest Sh value while 45 PP has the lowest over the Re range studied. Further, 45 PP has the strongest relationship with Re ( $Sh \propto Re^{0.323}$ ) while 90 HDPE shows weakest relationship ( $Sh \propto Re^{0.134}$ ). Our results vary from those reported in previous works: (Schock and Miquel, 1987) reported 0.875 and (Da Costa et al., 1994) reported 0.5 for the Re exponent for other commercial spacers, but this could be the result of different spacer geometries.

It appears that most geometries been optimized to maximize the exponent, which means that the spacer will get the greatest benefit from flow increases. On the other hand, as a result of the weak relation to flowrate, both 60 PP and 90 HDPE will lose a minimum of their performance from a reduction in flowrate. Overall, comparing the three spacer categories shows that Sh values for all of them are of the same order of magnitude.

Figure 6 plots Sh against Pn, thereby combining mass transfer and energy consumption results, and including previously reported data by (Kavianipour et al., 2017) and (Li et al., 2004). It serves to highlight the trade-off between production rate and energy costs. It should be noted that the rate of increase of Sh with Pn for the four commercial geometries studied herein is slower than reported by the literature performance envelopes. Figure 6 also shows that 60 PP and 90 HDPE have significantly higher mass transfer performance for Pn below around  $5 \times 10^6$ , compared to any of the other geometries studied. Based on Figure 6, 90 HDPE would be the best choice of spacer, as it delivers high Sh with a



relatively low energy requirement. While the  $Sh$  value of 60 PP is around 10% higher than that of 90 HDPE at the same  $Pn$ , its corresponding  $Re$  value is around 60% lower, meaning that 60 PP's production capacity is substantially lower.

Examination of the detailed CFD results could explain the behaviour of the 90 HDPE spacer. An explanation for the high mass transfer coefficient of the spacer for low flowrates, as well as its weak relationship with  $Re$ , is given in Section 3.2.

#### 3.1.4 Spacer Performance Ratio (SPMP)

Schwinge et al. (2002) defined and calculated SPMP for three filament configurations and three  $d/H$  values, but while the flowrate or  $Re$  is not clear, it is probable that they were generated for  $Re_{ch} = 200$ . On the other hand, there is no mention of a relationship between SPMP and  $Re$  by the authors. Table 4 shows the SPMP values reported by (Schwinge et al., 2002) alongside the SPMP' values calculated from our previously-reported and current work.

The study for different  $d/H$  values reveals that the Zigzag configuration is the best of the three geometries for all filament diameters. On the other hand, smaller filaments lead to better SPMP values in all cases (Schwinge et al., 2002). The difference between Zigzag / Cavity and Wavy / Ladder-type geometries is that the latter pair has longitudinal filaments that are absent in the former, while all the geometries have latitudinal filaments. The difference in values observed between (Schwinge et al., 2002) and our studies can be explained by the difference in bulk and wall solute concentration values (mass fractions of 0 and 1 in (Schwinge et al., 2002) compared to 0.05 and 0.35 in (Kavianipour et al., 2017), respectively) as well as our use of constant feed mass flowrate compared to constant  $Re$ . This issue has been already clarified in (Kavianipour et al., 2017).

Our study indicates that SPMP' does not vary in a consistent way with  $Re$  as shown in **Error! Reference source not found.** for seven different spacers. For different spacers, SPMP' might increase, decrease or do both with increasing  $Re$ . All the commercial spacers studied had very low values for SPMP'. All values presented in the current work are less than one and are in accordance with our previous results. This means that the Plain configuration, that is, a feed channel without any spacer, would be the best performing one among the spacers studied according to SPMP'.

#### 3.1.5 Spacer Configuration Efficacy (SCE)

As defined in (Saeed, 2012), SCE is the ratio of  $Sh$  to  $Pn$ , and it thus includes both the mass transfer and energy requirement characteristics of a spacer. As indicated in Figure 8, 90 HDPE has the highest SCE values over the  $Re$  range studied for the commercial spacers. In addition, it suffers a lower negative impact from increased flowrate as well (Table 2). Both behaviours can be explained by examining the detailed flow path and concentration polarization layer results around the filaments (Section 3.2).

The 45 PP and 90 PP spacers show the lowest SCE because of their high demand for energy and low mass transfer performance.

### 3.2. An insight into 90 HDPE

The 90 HDPE spacer would be best or second choice among commercial spacers, according to six different performance measures at both low and high flowrates (Section 3.3). In addition, **Error! Reference source not found.** Table 2 shows that the effect of flowrate on pressure drop and Sh is weaker than for the other configurations studied. Both phenomena can be explained by the physical configuration of 90 HDPE.

Figure 10 shows velocity and concentration contour plots for Re values of 50 and 200 for 90 HDPE. The velocity scales for the two Re plots were chosen to make the low and high flowrate plots visually comparable (Figure 9(a)). That is, the velocity scale for Re = 200 is four times higher than that for Re = 50, which is the same as the mass flowrate ratio, making the same colours represent the same ratio to the average velocity. On the other hand, for the concentration contour plots (Figure 9(b)), the maximum scale concentration was set to a value 1.5 times the weighted average outlet concentration. Logarithmic concentration scales were used to emphasise differences in the lower concentration ranges in both plots.

Examination of the circled area in Figure 9(a) shows different behaviour at low and high Re values. At low flow, most of the fluid goes through the wider gap and a low velocity zone is observed after the filament in the lower part of the channel. In contrast, at high flow, both wide and narrow gaps are almost equally used. The wider gap offers greater clearance, but a longer path, while the narrower gap has a shorter path, but with a smaller clearance. As visible in Figure 9(b), the concentration layer after the filament in the lower section of the channel for Re = 50 has been washed away at Re = 200, as indicated by the magnified region. The concentration plots also show that the small filaments are effective in depressing the concentration layers when they appear. Comparing the width and strength of the concentration layers around the thin and thick filaments indicates how effectively these small filaments can wash away rejected salts, reducing the osmotic pressure increase at the membrane surface and potentially also the deposition of scale.

Further investigation and possibly optimization in terms of  $L/H$  and  $d/H$  for thin and thick filaments and the number of thin filaments between thick filaments might lead to a better configuration.

### 3.3. Consistency of rankings obtained from alternative measures of spacer performance

The rankings of the commercial spacers, from best to poorest performing, based on the various performance measures ( $\Delta P/L$ , SPC, Pn, Sh, SPMP' and SCE), are shown in Figure 10 for low and high flowrates. For Re = 50, the pressure gradient and SPC are in full agreement. However, when it comes to Pn, 90 PP falls from first to third ranking. On the other hand, the three mass transfer measures are in partial agreement: 45 PP and 90 PP are ranked as the worst choices, while 60 PP and 90 HDPE are the best.

A similar result is observed for Re = 100 (Figure 10). There is agreement in the rankings for pressure gradient and SPC, as well as the same change in Pn observed for 90 PP, as explained above. The same partial agreement between SCE and Sh is displayed; 45 PP improves from being the worst choice according to SCE and Sh to being the second best by SPMP'.

**Error! Reference source not found.** shows the range of variation in the various performance measures among the different spacers at Re = 50 and 100 by presenting the ratio of the minimum to the maximum value. For example, at Re = 50, in terms of pressure drop, the best spacer has only 16% of the  $\Delta P/L$  of the worst spacer. The reported values of  $\Delta P/L$ , SPC, Pn, Sh and SCE are all in the same order of magnitude, while for SPMP' the variation can be up to three orders of magnitude. Comparison of the performance measure ratios at Re = 50 and 100 also reveals that (except for SPMP') they will not change

abruptly with flowrate, being only doubled or halved at most, as a result of a two-fold increase in the flowrate. For SPMP', however, the difference is as high as one order of magnitude.

To the best of the authors' knowledge, no other study has discussed the potential advantages and disadvantages, in terms of either consistency or sensitivity, of the results for different performance measures for feed spacers.

#### 4. Conclusions

In the current work, CFD investigations have been carried out to predict the effect of changes in flowrate on four commercial feed spacer configurations used in spiral wound modules in RO systems. Energy consumption and mass transfer of solute on the feed side are investigated through multiple performance measures including pressure drop, Specific Power Consumption, Power number, Sherwood number, modified Spacer Performance Ratio (SPMP') and Spacer Configuration Efficacy. The modelling approach validated in our previous work was used again in this study.

Based on the simulations, the following conclusions are drawn:

- Most of the performance measures were strongly affected by the Reynolds number, except for SPMP'.
- SPMP' did not vary in a consistent way with Reynolds number for the different spacers. Further attention is needed to define a flow-independent performance measure based on the SPMP' concept.
- Regression of the CFD results yielded good power law correlations for SCE, SPC and Pn as functions of Re. The correlations are very quick to apply and are in agreement with previous works (Da Costa et al., 1994; In Seok and Ho Nam, 1982; Kaviani-pour et al., 2017; Schock and Miquel, 1987).
- Different performance measures result in different spacer rankings for different Re values.
- SCE appears to be the preferred choice for the performance measure because it considers both mass transfer and energy consumption, and has predictable behaviour with Re, in contrast to the current definition of SPMP'.
- One of the four commercial spacers studied, the Naltex N05013\_90HDPE-NAT (90 HDPE) from DelStar Technologies, which ranked best or second best with respect to all measures, shows a surprisingly weak response to changes in flowrate, indicating the prospect of large energy savings with a small loss in mass transfer performance at low flowrates. Further studies required to provide optimum spacer design parameters.

## References

- Cipollina, A., Di Miceli, A., Koschikowski, J., Micale, G., Rizzuti, L., 2009. CFD simulation of a membrane distillation module channel. *Desalination and Water Treatment* 6, 177-183.
- Cipollina, A., Micale, G., Rizzuti, L., 2011. Membrane distillation heat transfer enhancement by CFD analysis of internal module geometry. *Desalination and Water Treatment* 25, 195-209.
- Da Costa, A.R., Fane, A.G., Wiley, D.E., 1994. Spacer characterization and pressure drop modelling in spacer-filled channels for ultrafiltration. *Journal of Membrane Science* 87, 79-98.
- Dashtpour, R., Al-Zubaidy, S., 2012. Energy Efficient Reverse Osmosis Desalination Process. *International Journal of Environmental Science and Development* 3, 339-345.
- Fimbres-Weihs, G.A., Wiley, D.E., 2007. Numerical study of mass transfer in three-dimensional spacer-filled narrow channels with steady flow. *Journal of Membrane Science* 306, 228-243.
- In Seok, K., Ho Nam, C., 1982. The effect of turbulence promoters on mass transfer - numerical analysis and flow visualization. *International Journal of Heat and Mass Transfer* 25, 1167-1181.
- Jon Johnson, M.B., 2009. Engineering Aspects of Reverse Osmosis Module Design. Lenntech, <http://www.lenntech.com/Data-sheets/Filmtec-System-Design-L.pdf>.
- Kavianipour, O., Ingram, G.D., Vuthaluru, H.B., 2017. Investigation into the effectiveness of feed spacer configurations for reverse osmosis membrane modules using Computational Fluid Dynamics. *Journal of Membrane Science* 526, 156-171.
- Li, F., Meindersma, G.W., de Haan, A.B., Reith, T., 2002a. Optimization of non-woven spacers by CFD and validation by experiments. *Desalination* 146, 209-212.
- Li, F., Meindersma, W., de Haan, A.B., Reith, T., 2002b. Optimization of commercial net spacers in spiral wound membrane modules. *Journal of Membrane Science* 208, 289-302.
- Li, F., Meindersma, W., de Haan, A.B., Reith, T., 2004. Experimental validation of CFD mass transfer simulations in flat channels with non-woven net spacers. *Journal of Membrane Science* 232, 19-30.
- Qureshi, M., Shakaib, M., 2013. CFD study for temperature and concentration profiles in membrane channels, International conference on Energy and Sustainability. NED University of Engineering & Technology, Karachi, Pakistan.
- Saeed, A., 2012. Effect of feed channel spacer geometry on hydrodynamics and mass transport in membrane modules, PhD Thesis in Chemical Engineering, Curtin University.
- Saeed, A., Vuthaluru, R., Vuthaluru, H., 2013. Concept of spacer configuration efficacy (SCE) applied to optimize ladder type feed spacer filament spacing in narrow channels, International Conference On Water Desalination, Treatment and Management & Indian Desalination Association Annual Congress, Jaipur, India: The Malaviya National Institute of Technology.
- Saeed, A., Vuthaluru, R., Vuthaluru, H.B., 2015a. Impact of Feed Spacer Filament Spacing on Mass Transport and Fouling Propensities of RO Membrane Surfaces. *Chemical Engineering Communications* 202, 634-646.
- Saeed, A., Vuthaluru, R., Vuthaluru, H.B., 2015b. Investigations into the effects of mass transport and flow dynamics of spacer filled membrane modules using CFD. *Chemical Engineering Research and Design* 93, 79-99.
- Saeed, A., Vuthaluru, R., Yang, Y., Vuthaluru, H.B., 2012. Effect of feed spacer arrangement on flow dynamics through spacer filled membranes. *Desalination* 285, 163-169.
- Santos, J.L.C., Geraldés, V., Velizarov, S., Crespo, J.G., 2007. Investigation of flow patterns and mass transfer in membrane module channels filled with flow-aligned spacers using computational fluid dynamics (CFD). *Journal of Membrane Science* 305, 103-117.

Schock, G., Miquel, A., 1987. Mass-Transfer and Pressure Loss in Spiral Wound Modules. *Desalination* 64, 339-352.

Schwinge, J., Wiley, D.E., Fletcher, D.F., 2002. Simulation of the flow around spacer filaments between channel walls. 2. Mass-transfer enhancement. *Industrial & Engineering Chemistry Research* 41, 4879-4888.

UNESCO, 2015. Encyclopedia of Desalination and Water Resources: Energy Requirements of Desalination Processes. DESWARE.NET, <http://www.desware.net/Energy-Requirements-Desalination-Processes.aspx>.

ACCEPTED MANUSCRIPT

Figure 1. Schematic diagrams of the feed spacer geometries considered in the present study.

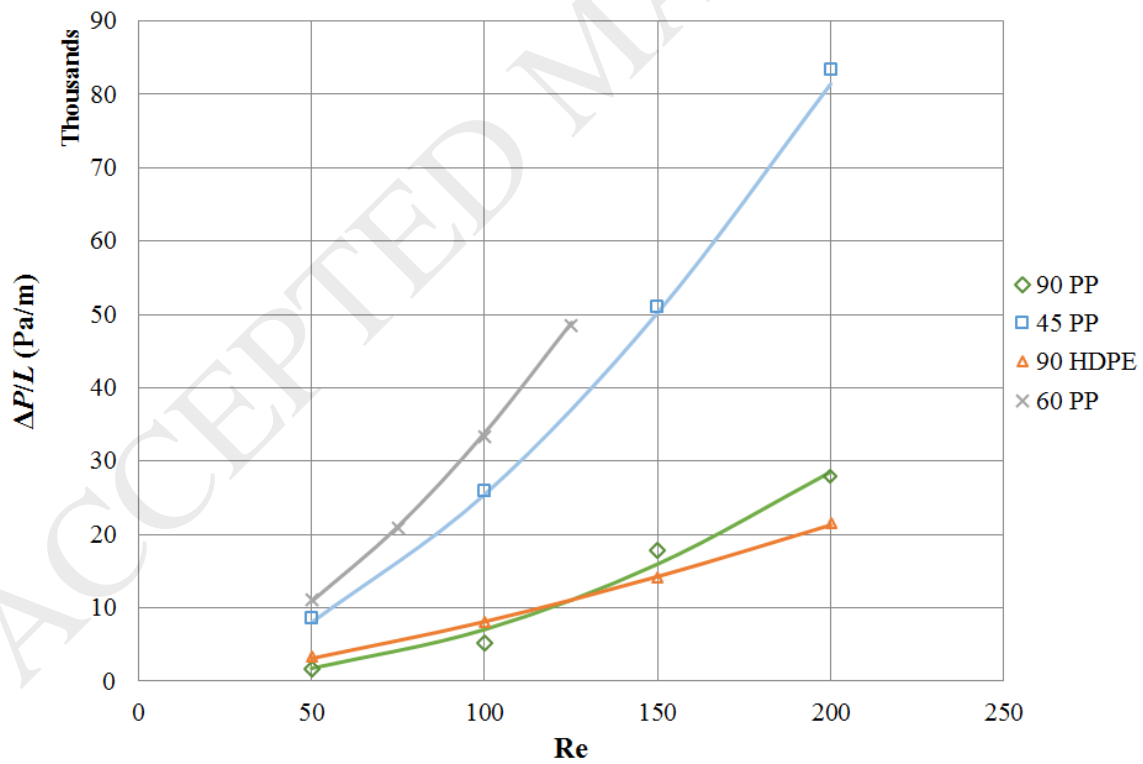
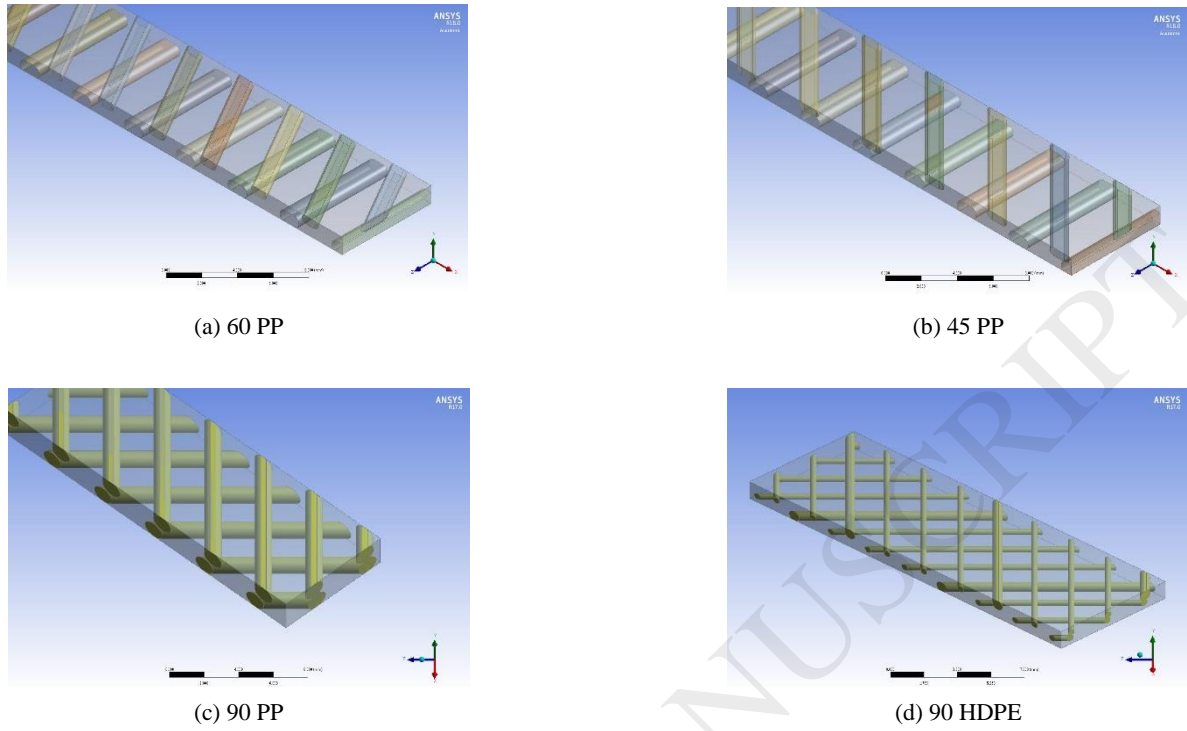
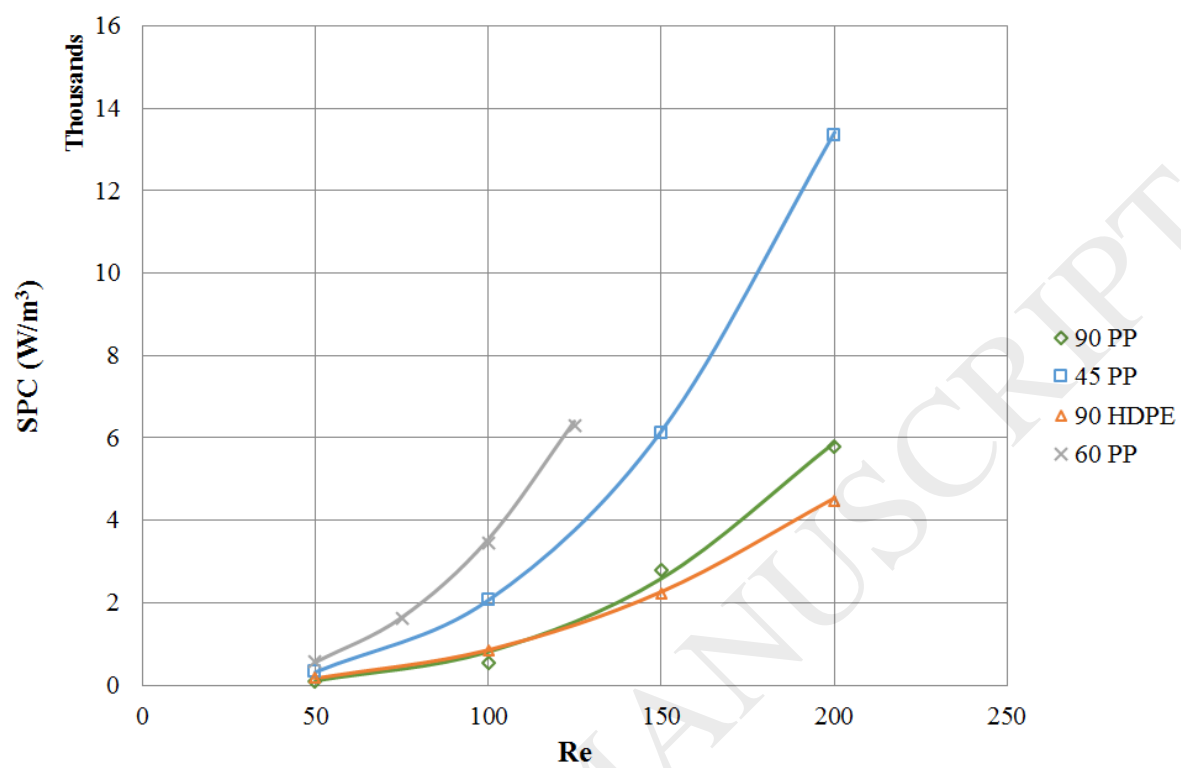


Figure 2. Predicted pressure drop per unit length as a function of  $Re$  for the four spacers.

Figure 3. Predicted Specific Power Consumption as a function of  $Re$  for the four spacers.



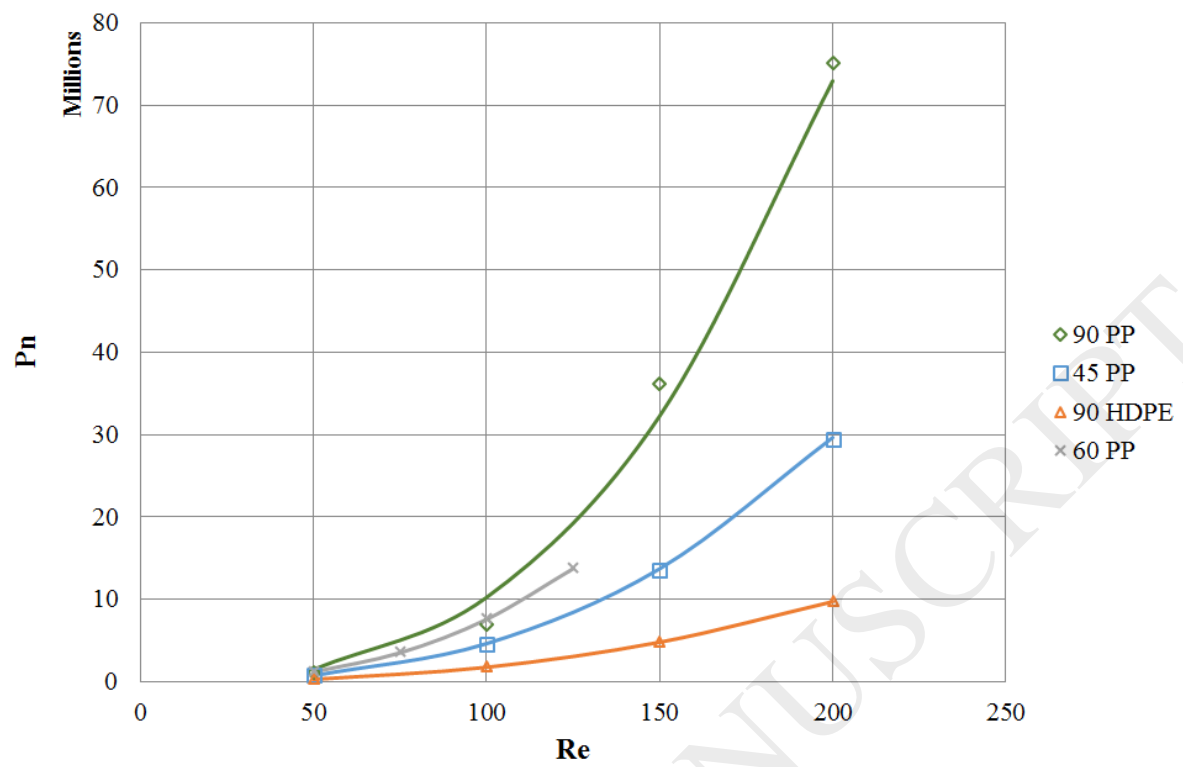


Figure 4. Predicted Power number as a function of Re for the four spacers.



Figure 5. Predicted Sherwood number as a function of  $Re$  for the four spacers.

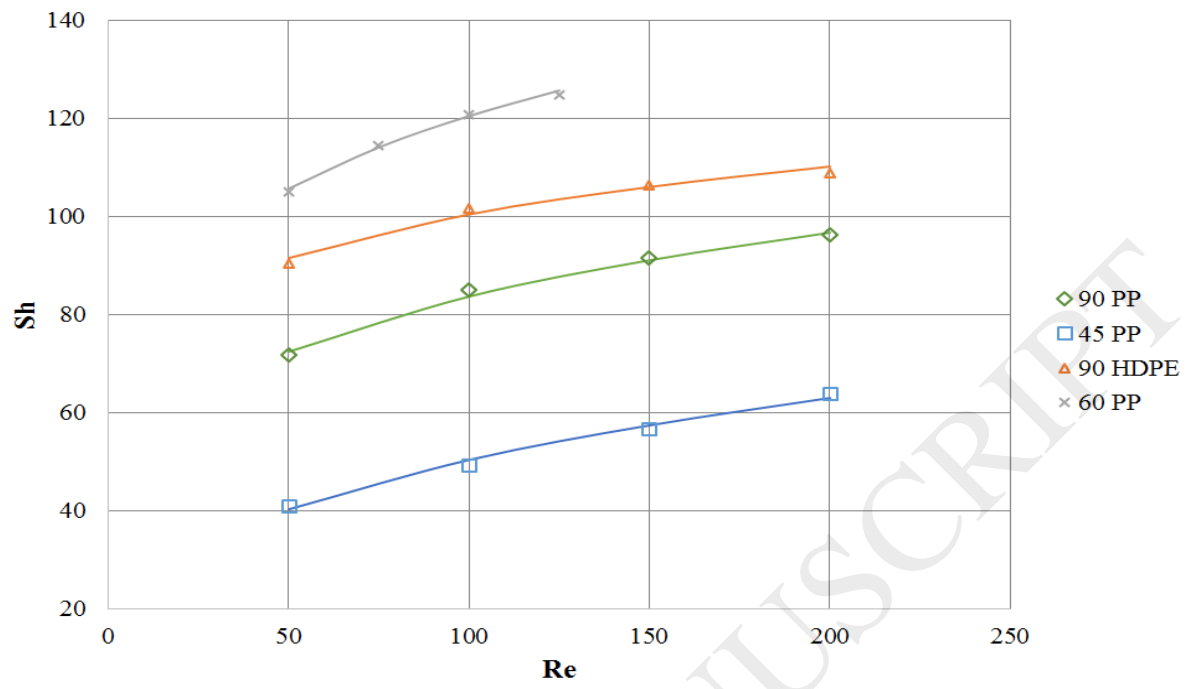


Figure 6. Trade-off between production capacity and energy consumption: Sherwood number as a function of Power number for the four commercial spacers and the results reported by (Li et al., 2004) and (Kavianipour et al., 2017).

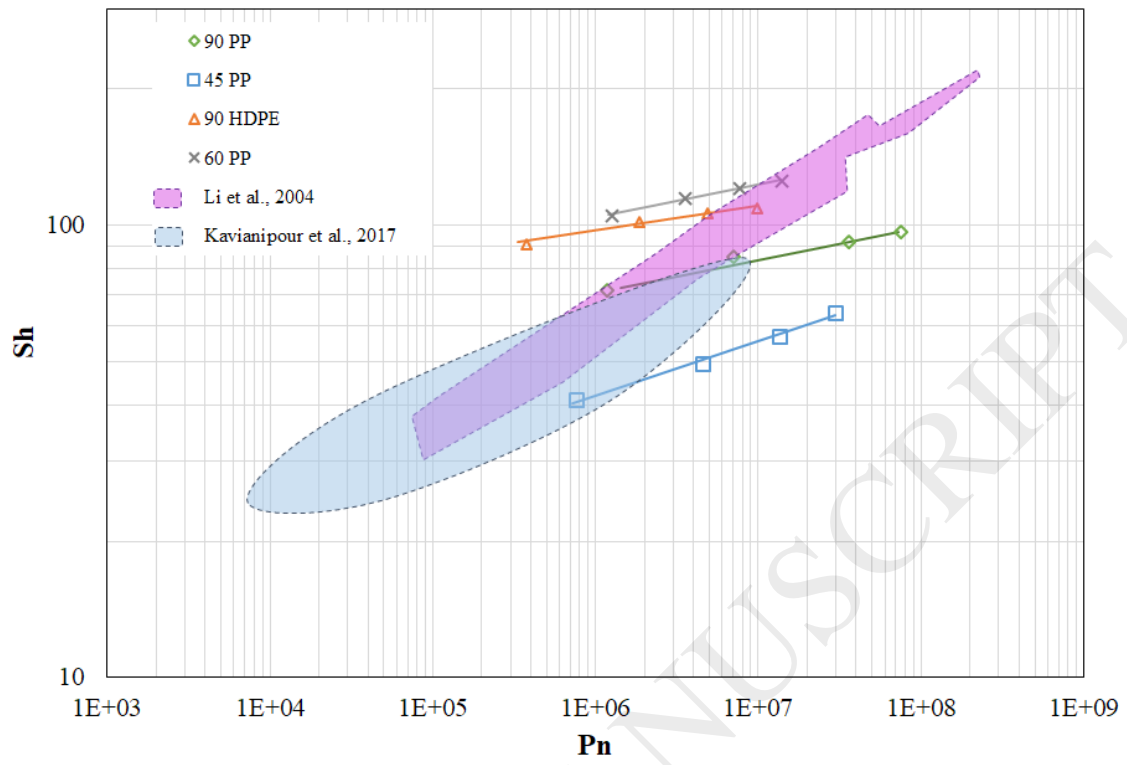


Figure 7. Predicted SPMP' as a function of Re for the four commercial spacers and three conventional spacer geometries studied in [19].

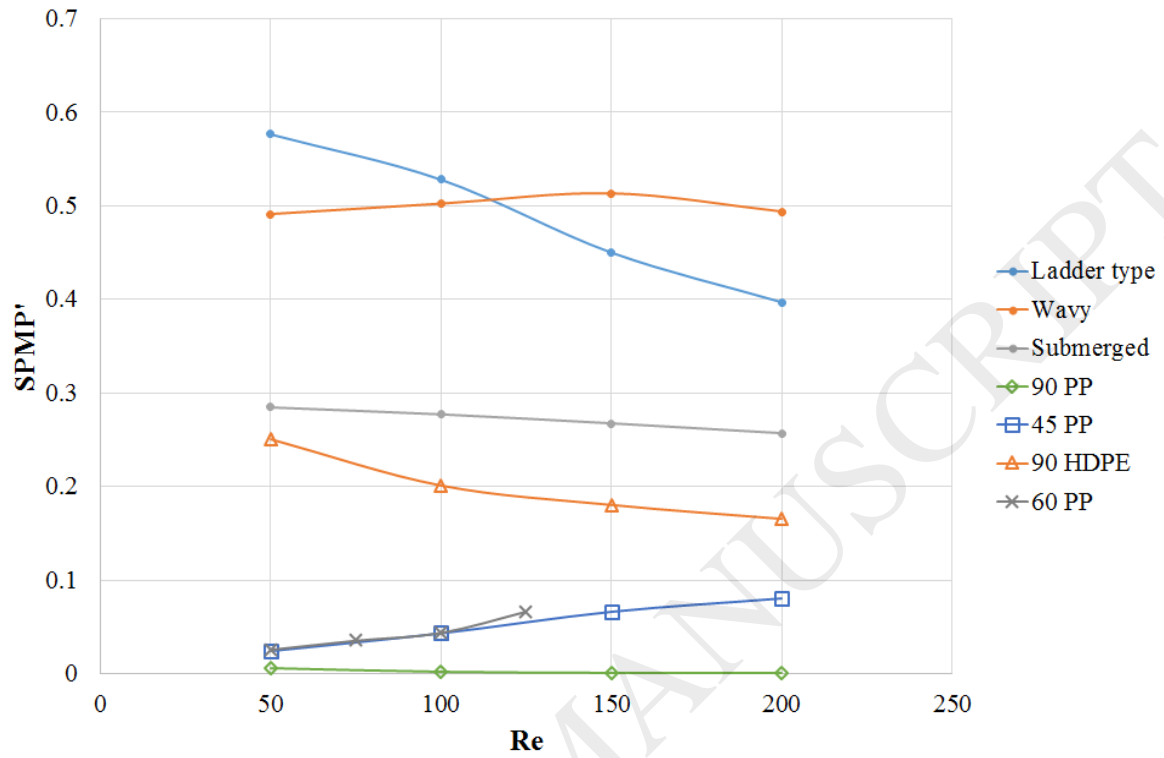


Figure 8. Predicted SCE as a function of Re for the four spacers.

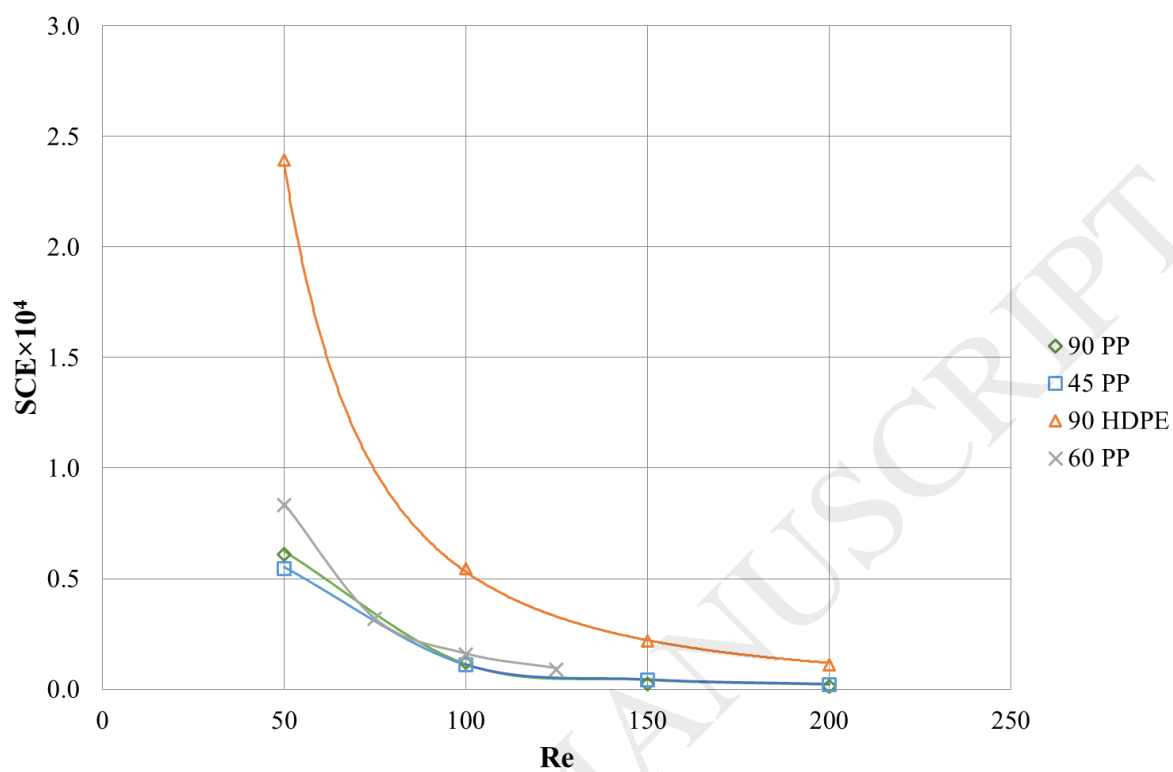
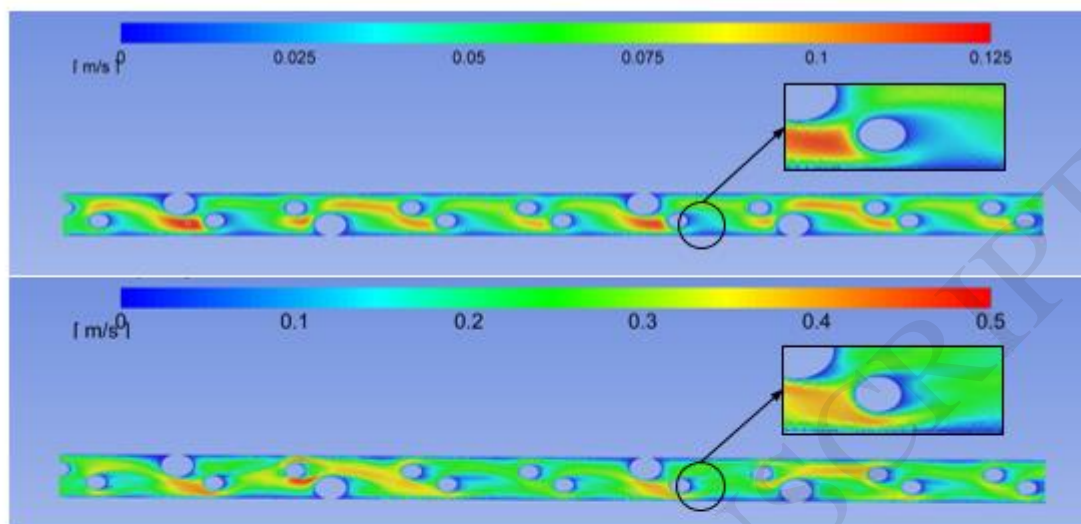
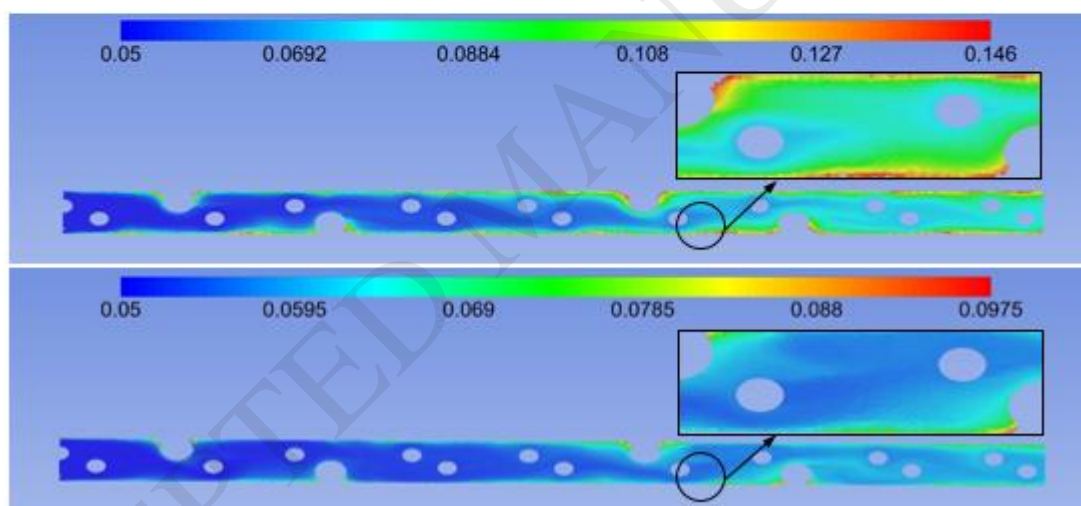


Figure 9. Contour plots for the 90 HDPE spacer.



(a) Velocity magnitude for  $Re \approx 50$  (top) and  $Re \approx 200$  (bottom). ¶



(b) Solute mass fraction for  $Re \approx 50$  (top) and  $Re \approx 200$  (bottom). Note that solute mass fractions higher than the upper limit of the colour scale are not shown in the solute contour plot. ¶

Figure 10. Spacer ranking using different performance measures (the outermost zone represents the best performance and the innermost zone the poorest performance).

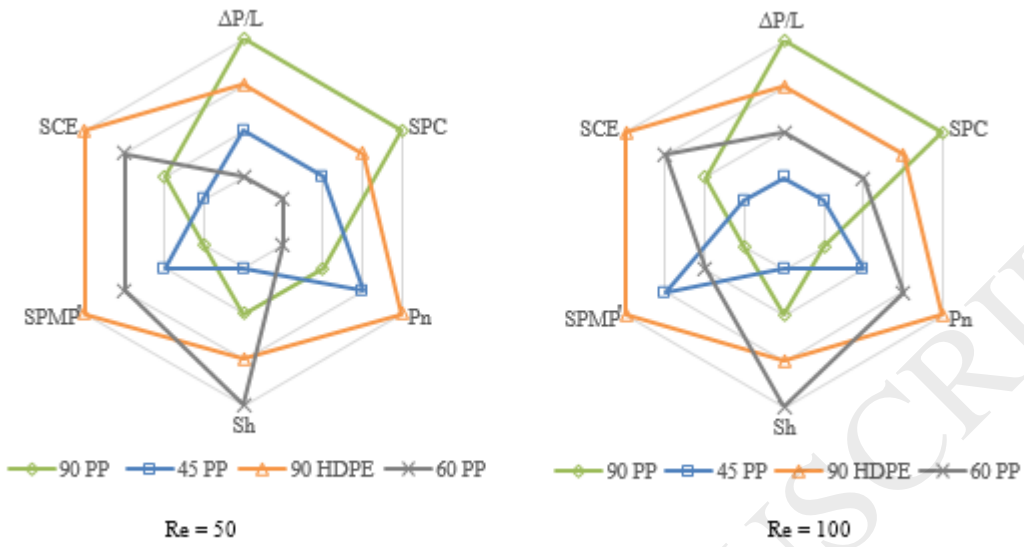


Table 1. Geometrical parameters of the spacers and CFD mesh size.

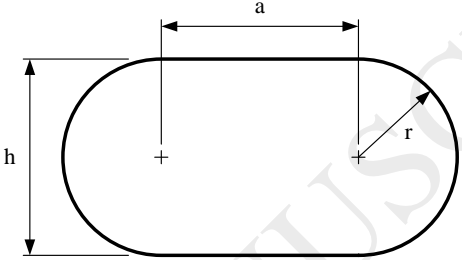
Configuration	90 PP	45 PP	90 HDPE	60 PP
Filament cross section shape	Circle	Discorectangle <sup>a</sup> $a = h = 2r$	Circle	Discorectangle <sup>a</sup> $a = h = 2r$
$D_h$ (mm)	1.74	1.25	1.14	1.24
$A_{eff}$ (mm <sup>2</sup> )	11.31	5.84	6.81	7.42
$\varepsilon$	0.772	0.681	0.883	0.865
Mesh size (number of elements)	16.2M	19.7M	10.7M	10.9M
<sup>a</sup> . Discorectangle shape and parameters 				

Table 2. Correlations for key variables derived from the current CFD simulations.

Configuration	90 PP	45 PP	90 HDPE	60 PP	Minimum R <sup>2</sup>
$\Delta P/L$ (Pa/m)	$0.640 \text{ Re}^{2.02}$	$11.1 \text{ Re}^{1.68}$	$13.5 \text{ Re}^{1.39}$	$17.6 \text{ Re}^{1.64}$	0.983
SPC (W/m <sup>3</sup> )	$1.63\text{E-}03 \text{ Re}^{2.85}$	$8.23\text{E-}03 \text{ Re}^{2.70}$	$1.23\text{E-}02 \text{ Re}^{2.42}$	$1.69\text{E-}02 \text{ Re}^{2.66}$	0.994
Pn	$21.3 \text{ Re}^{2.84}$	$20.2 \text{ Re}^{2.68}$	$24.9 \text{ Re}^{2.43}$	$36.5 \text{ Re}^{2.66}$	0.994
Sh	$32.2 \text{ Re}^{0.208}$	$11.4 \text{ Re}^{0.323}$	$54.2 \text{ Re}^{0.134}$	$50.5 \text{ Re}^{0.189}$	0.977
	$29.0 \text{ Pn}^{0.0665}$	$7.75 \text{ Pn}^{0.122}$	$44.1 \text{ Pn}^{0.0567}$	$38.4 \text{ Pn}^{0.0720}$	0.973
SPMP'	$7.08 \text{ Re}^{-1.84}$	$7.85\text{E-}4 \text{ Re}^{0.878}$	$0.806 \text{ Re}^{-0.300}$	$2.93 \text{ Re}^{1.11}$	0.944
SCE	$0.980 \text{ Re}^{-2.47}$	$0.503 \text{ Re}^{-2.33}$	$1.11 \text{ Re}^{-2.16}$	$0.930 \text{ Re}^{-2.38}$	0.998

Table 3. Correlations for selected key variables reported in (Kavianipour et al., 2017).

Configuration	Ladder-type	Triple	Wavy	Submerged	Minimum R <sup>2</sup>
$\Delta P/L$ (Pa/m)	$4.16 \text{ Re}^{1.49}$	$2.85 \text{ Re}^{1.55}$	$6.17 \text{ Re}^{1.37}$	$9.97 \text{ Re}^{1.29}$	0.9994
SPC (W/m <sup>3</sup> )	$2.69\text{E-}3 \text{ Re}^{2.52}$	$1.42 \text{ E-}3 \text{ Re}^{2.45}$	$4.20 \text{ E-}3 \text{ Re}^{2.40}$	$5.32 \text{ E-}3 \text{ Re}^{2.32}$	0.9999
Pn	$4.37 \text{ Re}^{2.42}$	$11.6 \text{ Re}^{2.48}$	$5.86 \text{ Re}^{2.33}$	$7.92 \text{ Re}^{2.24}$	0.9999
Sh	$10.1 \text{ Re}^{0.341}$	$8.43 \text{ Re}^{0.425}$	$3.62 \text{ Re}^{0.549}$	$5.85 \text{ Re}^{0.382}$	0.9743
	$8.96 \text{ Pn}^{0.140}$	$5.67 \text{ Pn}^{0.169}$	$2.44 \text{ Pn}^{0.234}$	$4.17 \text{ Pn}^{0.169}$	0.9690
SCE	$1.48 \text{ Re}^{-1.96}$	$0.419 \text{ Re}^{-1.93}$	$0.530 \text{ Re}^{-1.75}$	$0.640 \text{ Re}^{-1.83}$	0.9996



Table 4. Comparison of SPMP and SPMP' results.

Re	SPMP' based on (Kavianipour et al., 2017)			SPMP' from the current work				SPMP reported by (Schwinge et al., 2002)			
	Ladder-type	Wavy	Submerged	90 PP	45 PP	90 HDPE	60 PP	Spacer <i>d/H</i>	Zigzag	Cavity	Submerged
50	0.5768	0.4908	0.2846	0.0053	0.0242	0.2501	0.0258				
100	0.5282	0.5019	0.2771	0.0017	0.0433	0.2008	0.0355	0.3	3.45	2.80	1.11
150	0.4500	0.5128	0.2673	0.0006	0.0664	0.1801	0.0437	0.5	1.33	0.92	0.59
200	0.3967	0.4936	0.2567	0.0003	0.0808	0.1652	0.0663	0.7	0.89	0.54	0.28

ACCEPTED MANUSCRIPT

Table 5. Ratio of the minimum to maximum values of the indicated spacer performance measure at  $Re = 50$  and  $100$ .

Re	$\Delta P/L$	SPC	Pn	Sh	SPMP'	SCE
50	0.16	0.16	0.30	0.39	0.021	0.23
100	0.26	0.33	0.13	0.51	0.0017	0.12

ACCEPTED MANUSCRIPT